

Cardiovascular, Pulmonary and Renal Pathology

# High Glucose-Induced Thioredoxin-Interacting Protein in Renal Proximal Tubule Cells Is Independent of Transforming Growth Factor- $\beta$ 1

Weier Qi,<sup>\*†</sup> Xinming Chen,<sup>\* Richard E. Gilbert,<sup>†‡</sup>  
Yuan Zhang,<sup>†</sup> Mark Waltham,<sup>§</sup> Maria Schache,<sup>§</sup>  
Darren J. Kelly,<sup>†</sup> and Carol A. Pollock<sup>\*‡</sup></sup>

From the Department of Medicine,<sup>\*</sup> Kolling Institute, Royal North Shore Hospital and University of Sydney, Sydney, New South Wales, Australia; the Department of Medicine,<sup>†</sup> St. Vincent's Hospital, Melbourne, Victoria, Australia; St. Vincent's Institute of Medical Research,<sup>§</sup> Melbourne, Victoria, Australia; and the Department of Medicine,<sup>‡</sup> University of Toronto, St. Michael's Hospital, Toronto, Ontario, Canada

**Hyperglycemia is a causative factor in the pathogenesis of diabetic nephropathy. Here, we demonstrate the transcriptional profiles of the human proximal tubule cell line (HK-2 cells) exposed to high glucose using cDNA microarray analysis. Thioredoxin-interacting protein (Txnip) was the gene most significantly increased among 10 strongly up-regulated and 15 down-regulated genes. Txnip, heat shock proteins 70 and 90, chemokine (C-C motif) ligand 20, and matrix metalloproteinase-7 were chosen for verification of gene expression. Real-time reverse transcriptase-polymerase chain reaction confirmed the mRNA expression levels of these five genes, consistent with microarray analysis. The increased protein expression of Txnip, CCL20, and MMP7 were also verified by Western blotting and enzyme-linked immunosorbent assay. Increased expression of Txnip and of nitrotyrosine, as a marker of oxidative stress, were confirmed *in vivo* in diabetic Ren-2 rats. Subsequent studies focused on the dependence of Txnip expression on up-regulation of transforming growth factor (TGF)- $\beta$ 1 under high-glucose conditions. Overexpression of Txnip and up-regulation of Txnip promoter activity were observed in cells in which the TGF- $\beta$ 1 gene was silenced in HK-2 cells using short interfering RNA technology. High glucose further increased both Txnip expression and its promoter activity in TGF- $\beta$ 1 silenced cells compared with wild-type cells exposed to high glucose, suggesting that high glucose induced Txnip through a TGF- $\beta$ 1-indepen-**

**dent pathway. (Am J Pathol 2007, 171:744–754; DOI: 10.2353/ajpath.2007.060813)**

Hyperglycemia is recognized to be the key factor driving renal functional and pathological changes in diabetic nephropathy. However, the molecular mechanisms underpinning the development of nephropathy are complicated because of multiplicity of genetic, biochemical, and hormonal abnormalities coexisting in patients with either type I or type II diabetes mellitus. Proximal tubule cells constitute the bulk of the renal cortical cells and their central role in tubulointerstitial injury in diabetic nephropathy has been extensively studied.<sup>1,2</sup> Hence the proximal tubule cells are an ideal model in which to unravel the cellular mechanisms underpinning the tubulointerstitial changes in diabetic nephropathy that ultimately predict a progressive decline in renal function. Furthermore, we and others<sup>3,4</sup> have determined that exposure of these cells to elevated glucose concentrations has an important priming effect on the cells that may facilitate the generation of a profibrotic response.

Reactive oxygen species (ROS) are produced by various stressors as well as endogenous metabolic activities, including glucose metabolism. High glucose-induced ROS have been directly implicated in diabetic nephropathy. Thioredoxin functions as a cellular antioxidant, whereas thioredoxin interacting protein (Txnip), also known as vitamin D<sub>3</sub> up-regulated protein-1 or thioredoxin binding protein-2, is the endogenous inhibitor of cellular thioredoxin, inactivating its anti-oxidative function by binding to the redox-active cysteine residues. The

---

Supported by the National Health and Medical Research Council (post-doctoral fellowship to W.Q.) and the Juvenile Diabetes Research Foundation (international career development award to D.J.K.).

W.Q. and X.C. contributed equally to this study.

Accepted for publication April 16, 2007.

Address reprint requests to Professor Carol A. Pollock, Dept. of Medicine, Level 3, Wallace Freeborn Professorial Block, Royal North Shore Hospital, St. Leonards, NSW, Australia 2065 or Dr. Weier Qi, Dept. of Medicine, St. Vincent's Hospital, Fitzroy, VIC 3065, Australia. E-mail: carpol@med.usyd.edu.au and wqi@medstv.unimelb.edu.au.

Txnip gene is located on human chromosome 1q21, a region with a high frequency of genomic instability, and it expresses a 46-kd protein ubiquitously present in many tissues. It has recently been recognized in vascular tissues that hyperglycemia promotes oxidative stress through inhibition of thioredoxin function by increased expression and activity of Txnip,<sup>5</sup> leading to a functional inhibition of anti-oxidative thioredoxin function. This specific interaction results in a shift of the cellular redox balance that promotes increased intracellular oxidative stress.<sup>6,7</sup>

Transforming growth factor (TGF)- $\beta$ 1 is a well-recognized profibrotic and inflammatory cytokine in the kidney playing a central role in progressive kidney diseases including diabetic nephropathy.<sup>8–10</sup> TGF- $\beta$ 1 has been reported to generate ROS in NRK-52E cells, rat immortalized renal proximal tubular cells, and Mv1Lu cells.<sup>11–13</sup> However, the role of TGF- $\beta$ 1 in regulating Txnip expression is unknown.

The aim of this work was firstly to determine the transcriptional profiles of human proximal tubule cell line (HK-2 cells) exposed to prolonged high glucose using cDNA microarray technology. Txnip was the gene highly induced by high glucose. Hence, further studies were done to determine the *in vivo* expression levels of ROS and Txnip in diabetic Ren-2 rats and the role of TGF- $\beta$ 1 on the expression of Txnip and its promoter activity under high-glucose conditions.

## Materials and Methods

### Cell Culture

HK-2 cells, a proximal tubule cell line from American Type Cell Collection (Rockville, MD), were used in this study. HK-2 cells were 10% subconfluent when seeded on 10-cm Petri dishes and cells were maintained in medium containing 5 or 30 mmol/L D-glucose or 30 mmol/L L-glucose for 11 days. Medium was changed every 2 days to maintain glucose levels in the desired range. On day 10, 10 ml of treatment medium was added to each 10-cm Petri dish. Conditioned media were collected on day 11 and centrifuged at 3000 rpm and 4°C for 10 minutes to remove cell debris and then stored at -80°C for measurement of CCL20 and MMP7 protein levels using enzyme-linked immunosorbent assay (R&D Systems, Minneapolis, MN). RNA was collected for cDNA microarray analysis and verification of interested gene expression. Cell lysate was collected for measurement of Txnip protein level using Western blotting. To determine the levels of Txnip mRNA expression at different time points, HK-2 cells were 10% subconfluent when seeded onto a six-well plate, and cells were maintained in medium containing 5 and 30 mmol/L D-glucose. RNA was collected on days 1, 2, 4, and 11 after HK-2 cells were exposed to 5 and 30 mmol/L D-glucose. HK-2 cells were exposed to 10 ng/ml TGF- $\beta$ 1 for 0, 1, 2, 4, and 6 days, and Txnip mRNA and protein expression were measured by real-time reverse transcriptase-polymerase chain reaction (RT-PCR) and Western blotting.

Thirty nmol/L TGF- $\beta$ 1 short interfering RNA (siRNA) (Ambion, Austin, TX) was introduced into HK-2 cells using Lipofectamine 2000 (Invitrogen, Carlsbad, CA) according to the manufacturer's instructions. In parallel, cells were transfected with 30 nmol/L of nonspecific siRNA, which served as the control data set. Cells were then treated with or without 30 mmol/L D-glucose for 72 hours. RNA was extracted using RNeasy mini kit (Qiagen, Valencia, CA) and cell lysate was collected for the measurement of Txnip mRNA and protein expression. To determine further if TGF- $\beta$ 2 and TGF- $\beta$ 3 account for the increased Txnip in TGF- $\beta$ 1 silenced cells, HK-2 cells were transfected with TGF- $\beta$ 1 siRNA and 30  $\mu$ g/ml of pan-specific TGF- $\beta$  antibody or rabbit IgG as negative control (R&D Systems) was added 6 hours after transfection. Cell lysate was collected at 24 hours for measurement of Txnip protein.

### cDNA Microarray Analysis

On day 11, when cells were maintained in medium containing 5 and 30 mmol/L D-glucose or 30 mmol/L L-glucose as described above in the cell culture section, supernatant was removed and cells were washed once in phosphate-buffered saline (PBS). Total RNA was extracted using TRIzol reagent (Invitrogen) and cleaned up with RNeasy mini kit (Qiagen) according to the manufacturer's instructions. Intact RNA was analyzed through 1.5% denaturing agarose gel. Poly(A)-containing RNA was purified from total RNA using the Oligotex mRNA midikit (Qiagen) and quantified using the Ribo-Green RNA quantification kit (Molecular Probes, Eugene, OR). Complementary DNAs were then generated from mRNAs obtained from treated and control cells and labeled with Cy3 and Cy5 fluorescent dyes, respectively, in one experiment and with the dyes in reverse in a second experiment. Fluorescent-labeled cDNAs were hybridized to the gene chips (Compugen 19k v. 3), which consisted of 19,000 genes (Clive and Vera Ramaciotti Centre, Sydney, NSW, Australia). The sample labeling and hybridization were repeated once. Microarray analysis was performed in Microarray Workstation at the Pharmacogenomics Unit at St. Vincent's Hospital, Melbourne, VIC, Australia. The slides were scanned on Gene Pix 4000A Axon scanner (Axon Instruments, Sunnyvale, CA). A confocal microscope attached to a detector system recorded the emitted light from each of the microarray spot, allowing high-resolution detection of the hybridization signals. The raw data were generated with Microarray Image Analysis software GenePix Pro 6.0 (Axon Instruments). Acuity 4.0 software (Axon Instruments) was used for data analysis such as normalization, statistical analysis, and filtering.

### Real-Time RT-PCR

Real-time PCR after reverse transcription was used to assess transcript levels of Txnip, HSP70, HSP90, CCL20, and MMP-7. Both water blank and nonreverse-transcribed RNA samples were used as negative controls. Briefly, total RNA (2  $\mu$ g) was treated with DNase I (In-

**Table 1.** Real-Time RT-PCR Primers

Gene name	Accession no.	Sense	Anti-sense	Size (bp)
<i>TXNIP</i>	NM_006472	5'-CGCCACACTTACCTTGCCAATG-3'	5'-GCTCTTGCCACGCCATGATG-3'	111
<i>HSP70</i>	NM_006597	5'-CAGGGAAACCGAACCACT-3'	5'-ATTCTTTGCGGCATCACC-3'	75
<i>HSP90</i>	X15183	5'-CAGAGCCCTTCTATTTGT-3'	5'-ATCCTCCGAGTCTACCAC-3'	169
<i>CCL20</i>	NM_004591	5'-AGAGTTTGCTCCTGGCTG-3'	5'-GGATGAAGAATACGGTCTGTG-3'	114
<i>MMP7</i>	Z11887	5'-GGATGGTAGCAGTCTAGGGATTA-3'	5'-GGAATGTCCCATACCCAAAGAA-3'	79
<i>β-Actin</i>	AY582799	5'-ATCGTGCCTGACATTAAG-3'	5'-ATTGCCAATGGTGATGAC-3'	135

vitrogen), and then cDNA was synthesized using reverse transcriptase Superscript II RT (Invitrogen). Specific primers for the use of SYBR Green are shown in Table 1. Primer specificity in real-time PCR reactions was confirmed using RT-PCR. A 25- $\mu$ l real-time PCR reaction included Brilliant SYBR Green QRT-PCR Master Mix according to the manufacturer's instructions (Stratagene, La Jolla, CA). Real-time quantitations were performed on the iCycler iQ system (Bio-Rad, Hercules, CA). The fluorescence threshold value was calculated using the iCycle iQ system software. The calculation of relative change in mRNA was performed using the delta-delta method,<sup>14</sup> with normalization for the housekeeping gene  $\beta$ -actin.

#### *CCL20 and MMP-7 Enzyme-Linked Immunosorbent Assay*

Conditioned media were collected and centrifuged at 3000 rpm and 4°C for 10 minutes to remove cell debris and then stored at -80°C. CCL20 and MMP7 were quantified using enzyme-linked immunosorbent assays (R&D Systems) according to the manufacturer's instructions.

#### *In Vivo Studies in Diabetic Ren-2 Rats*

Eight-week old female, homozygous (mRen-2)27 rats (St. Vincent's Hospital Animal House, Melbourne, Australia) weighing 170  $\pm$  20 g were randomized to receive either 55 mg/kg streptozotocin (Sigma, St. Louis, MO) diluted in 0.1 mol/L citrate buffer, pH 4.5, or citrate buffer (nondiabetic) by tail vein injection after an overnight fast.<sup>8,15</sup> Each week, rats were weighed, their blood glucose was determined using an AMES glucometer (Bayer Diagnostics, Melbourne, VIC, Australia), and only streptozotocin-treated animals with blood glucose >20 mmol/L were considered diabetic. Every 4 weeks, systolic blood pressure was determined in preheated conscious rats via tail-cuff plethysmography using a noninvasive blood pressure controller and Powerlab (AD Instruments, Bella Vista, NSW, Australia). All animals were housed in a stable environment maintained at 22  $\pm$  1°C with a 12-hour light/dark cycle commencing at 6 AM. Diabetic rats received twice a week injection of insulin (2 to 4 U i.p., Humulin NPH; Eli Lilly and Co., Indianapolis, IN) to reduce mortality and to promote weight gain. Experimental procedures adhered to the guidelines of the National Health and Medical Research Council of Australia's Code for the Care and Use of Animals for Scientific Purposes and were approved by the Animal Research Ethics Committee of St. Vincent's Hospital.

#### *Tissue Preparation and Immunohistochemistry*

Rats were anesthetized (Nembutal, 60 mg/kg body weight i.p.; Boehringer-Ingelheim, Sydney, NSW, Australia) and the abdominal aorta cannulated with an 18-gauge needle. Perfusion-exsanguination commenced at systolic blood pressure (180 to 220 mmHg) via the abdominal aorta with 0.1 mol/L PBS, pH 7.4 (20 to 50 ml) to remove circulating blood, and the inferior vena cava adjacent to the renal vein was simultaneously severed allowing free flow of the perfusate. After clearance of circulating blood, 4% paraformaldehyde in 0.1 mol/L phosphate buffer, pH 7.4, was perfused for a further 5 minutes (100 to 200 ml of fixative). Kidneys were then excised, decapsulated, sliced transversely, immersed into 4% paraformaldehyde in 0.1 mol/L phosphate buffer for overnight fixation, and then paraffin-embedded for subsequent light microscopic evaluation.<sup>8</sup>

#### *Immunohistochemistry for Nitrotyrosine and TXNIP*

In brief, 4- $\mu$ m tissue sections were placed into histosol to remove the paraffin wax, rehydrated in graded ethanol, and immersed into tap water before being incubated for 20 minutes with normal swine serum diluted 1:10 with 0.1 mol/L PBS, pH 7.4. Sections were then incubated with rabbit anti-nitrotyrosine (Upstate Technology, Lake Placid, NY) diluted 1:500 with PBS and anti-Txnip (Zymed Laboratories, South San Francisco, CA) diluted 1:50 overnight (18 hours) at 4°C. The following day the sections were thoroughly washed in PBS (3  $\times$  5 minute changes), incubated with 3% hydrogen peroxide for 10 minutes to block endogenous peroxidase, then rinsed with PBS (2  $\times$  5 minutes), and incubated with biotinylated swine anti-rabbit IgG antibody (DAKO, Carpinteria, CA), diluted 1:200 with PBS. Sections were rinsed with PBS (2  $\times$  5 minutes) followed by incubation with an avidin-biotin peroxidase complex (Vector Laboratories, Burlingame, CA), diluted 1:200 with PBS. After rinsing with PBS (2  $\times$  5 minutes), localization of the peroxidase conjugates was achieved by using diaminobenzidine tetrahydrochloride as a chromogen, for 1 to 3 minutes. Sections were rinsed in tap water for 5 minutes to stop reaction and then counterstained in Mayer's hematoxylin, differentiated in Scott's tap water, dehydrated, cleared, and mounted in Depex. Sections incubated with 1:10 normal swine serum, instead of the primary antiserum, served as the negative controls.<sup>8</sup> All of the slides were blinded, and five random nonoverlapping fields from three rats in each experimental group were chosen. The positive immuno-

staining of ROS and Txnip in dilated tubules was counted separately and normalized to the total tubules counted in each chosen field.

### Txnip Western Blotting

Western blotting was performed on cell lysate collected from HK-2 cells and whole rat kidney tissue for detection of Txnip. In brief, equal amounts of protein from each sample were subjected to sodium dodecyl sulfate-polyacrylamide gel electrophoresis under reducing conditions. Proteins were then transferred to Hybond ECL nitrocellulose membrane (Amersham Pharmacia Biotech, Buckinghamshire, UK). Nonspecific binding sites were blocked for 1 hour (5% nonfat milk and 0.1% Tween 20 in PBS) after which the membranes were exposed to Txnip primary antibody at a concentration of 3  $\mu$ g/ml in 5% nonfat milk and 0.1% Tween 20 in PBS (Zymed Laboratories) overnight at 4°C, followed by washing four times, after which they were incubated with peroxidase-labeled secondary antibodies (Amersham Pharmacia Biotech) for 1 hour and again washed four times. The blots were then detected using enhanced chemiluminescence (Amersham Pharmacia Biotech). The bands corresponding to Txnip (46 kd) were quantitated using gel documentation (Bio-Rad) and quantitated by densitometry using Quantity One software (Bio-Rad). Coomassie Brilliant Blue staining was used to confirm that an equal amount of protein was loaded in each lane.

### Txnip Promoter Activity Assay

The promoter activity of Txnip was determined by Dual-Luciferase reporter assay system (Promega, Madison, WI). The promoter sequence of Txnip was designed and amplified using GC-2 PCR kit (BD Biosciences, San Diego, CA). The DNA fragment of Txnip promoter was cloned into pGL3 firefly luciferase Vector (Promega). The plasmid containing the Txnip promoter sequence was introduced into HK-2 cells using Lipofectamine 2000. As a negative control, pGL3-Basic vector with no promoter inserted was transfected into the cells. pRL-SV40 Renilla vector (Promega) was co-transfected into cells, and its luciferase activity was used for normalization of transfection efficiency. Luciferase activity was detected with a 20/20n luminometry system with dual autoinjector (Promega).

### Statistical Analysis

All results are expressed as a fold change compared with the control value. Each experiment was performed independently a minimum of three times. Results are expressed as mean  $\pm$  SEM. Statistical comparisons between groups were made by analysis of variance, with pairwise multiple comparisons made by Fisher's protected least-significant difference test. Analyses were performed using the software package, Statview version 4.5 (Abacus Concepts Inc., Berkeley, CA). *P* values less than 0.05 were considered significant.

**Table 2.** Genes Undergoing Most Striking Up-Regulation and Down-Regulation after HK-2 Cells Were Exposed to High Glucose for 11 Days in cDNA Microarray Analysis

Name	Accession no.	Fold change (Cy5/Cy3)	Fold change (Cy3/Cy5)	Gene symbol
<b>Down-regulated genes</b>				
<i>Homo sapiens</i> PUMP-1 gene encoding PUMP	Z11887	4.0627	5.0339	MMP-7
<i>H. sapiens</i> crystallin, $\mu$ (CRYM) mRNA	NM_001888	2.2503	2.5798	CRYM
<i>H. sapiens</i> cDNA FLJ10500 fis, clone NT	AK001362	2.2929	2.4311	L2HGDH
<i>H. sapiens</i> protein tyrosine phosphatase	NM_002829	2.1629	2.3910	PTPN3
Human HepG2 3' region cDNA, clone hmd1b1	D16856	2.2327	2.3069	HMD1B10
<i>H. sapiens</i> clusterin (complement lysis inhibitor)	NM_001831	2.5188	2.2404	APOJ, clusterin
<i>H. sapiens</i> solute carrier family 4	NM_003759	1.9691	2.2241	SLC4A4
<i>H. sapiens</i> Ras-related associated with diabetes	NM_004165	2.0304	2.1757	RRAD
<i>H. sapiens</i> secreted phosphoprotein 1	NM_000582	2.2614	2.1739	SPP1
<i>H. sapiens</i> <i>N</i> -acylsphingosine amidohydrolase	NM_004315	2.2597	2.1343	ASAH1
<i>H. sapiens</i> serpin peptidase inhibitor	NM_000295	2.4027	2.1251	SERPINA1
<i>H. sapiens</i> signal transducer and activator of transcription 1, 91 kd (STAT1)	NM_007315	1.9253	2.1027	STAT1
<i>Homo sapiens</i> KIAA0977 protein (KIAA0977)	NM_014900	1.9847	2.0635	COBLL1
Human $\alpha$ -1-antitrypsin ( $\alpha$ -1-AT)	M26123	2.3010	2.0072	SERPINA1
<i>H. sapiens</i> insulin-like growth factor	NM_001553	2.0164	1.9455	IGFBP7
<b>Up-regulated genes</b>				
<i>H. sapiens</i> up-regulated by 1,25-dihydro	NM_006472	12.1736	11.2292	TXNIP
<i>H. sapiens</i> chemokine (C-C motif) ligand 20	NM_004591	4.3665	6.2174	CCL20, MIP3A_
<i>H. sapiens</i> transferrin receptor (p90, CD71) (TFRC)	NM_003234	3.8612	3.9039	TFRC, TRFR_
<i>H. sapiens</i> heat shock 70-kd protein	NM_006597	2.8836	2.8227	HSPA8
<i>H. sapiens</i> G $\alpha$ /G $\beta$ switch 2 (G0S2)	NM_015714	2.3696	2.7238	HSD11B1
Human plasminogen activator inhibitor-1	M16006	2.2150	2.3579	PAI-1
<i>H. sapiens</i> angiopoietin-like 4 (ANGPTL4)	NM_016109	2.8786	2.3457	ANGPTL4
Human mRNA for 90-kd heat-shock protein	X15183	2.2072	2.3411	HSPCA
<i>H. sapiens</i> heat shock 105 kd (HSP105B)	NM_006644	2.0881	2.0406	HSPH1
<i>H. sapiens</i> tissue factor pathway inhibitor 2 (TFPI2)	NM_006528	2.7032	2.0056	TFPI2

## Results

### Transcriptional Profiles of HK-2 Cells Exposed to High Glucose for 11 Days

cDNA microarray analysis was performed on samples from HK-2 cells exposed to high glucose for 11 days. A twofold change was considered as a threshold for real differences in gene expression change. Fifteen down-regulated and 10 up-regulated genes were identified (Table 2). Among these genes, Txnip, HSP70, HSP90, CCL20, and MMP-7 were chosen for further study.

Txnip was found to be the gene most significantly up-regulated in the cDNA microarray analysis. High glucose increased Txnip mRNA expression more than 50-fold after HK-2 cells were exposed to high glucose for 11 days by real-time RT-PCR ( $P < 0.0005$ ) (Figure 1A) with significant increase in Txnip protein expression (Figure 1, B and C). High glucose increased Txnip from day 1 and had a striking increase on day 11, suggesting chronic hyperglycemia promoted the induction of Txnip expression (Figure 1D).

Two stress-related genes, heat shock protein 70 and 90 (HSP70 and HSP90), were found to increase significantly when exposed to prolonged high glucose in microarray analysis. These data were confirmed using real-time RT-PCR. Both HSP70 and HSP90 increased more than threefold after HK-2 cells exposure to high glucose for 11 days (both  $P < 0.0005$ ) (Figure 2, A and B).

CCL20 mRNA expression increased 20-fold after exposure of HK-2 cells to high glucose for 11 days ( $P < 0.0005$ ) (Figure 2C). Protein level of CCL20 also increased ( $P < 0.005$ ) (Figure 2D). MMP-7 mRNA expression decreased to 0.1-fold after exposure of HK-2 cells to high glucose for 11 days ( $P < 0.0005$ ) (Figure 2E). Protein level of MMP-7 decreased by 90% ( $P < 0.0005$ ) (Figure 2F). Exposure to the osmotic control (30 mmol/L L-glucose) did not change the expression levels of Txnip, HSP70, HSP90, CCL20, and MMP-7. These data suggested that the high glucose-induced changes in these genes were not attributable to osmotic stress on the cells but specific to the high extracellular glucose concentrations. Table 3 compares the results between cDNA microarray analysis and real-time RT-PCR for gene expression of Txnip, HSP70, HSP90, CCL20, and MMP-7 in HK-2 cells exposed to high glucose for 11 days.

### The Levels of ROS Generation and Txnip Significantly Increased in Diabetic Ren-2 Rats

Transgenic Ren-2 rats rendered diabetic with streptozotocin<sup>8,15</sup> were used as an *in vivo* model to assess the degree of ROS production and Txnip in a model of progressive diabetic nephropathy. The animal characteristics are shown in Table 4. The transgenic Ren-2 rat develops many of the structural and functional manifestations of diabetic nephropathy. These include hypertension, albuminuria, declining glomerular filtration rate, severe glomerulosclerosis, and florid tubulointerstitial disease.<sup>8,15</sup> Nitrotyrosine was chosen as a marker of intracellular ROS. Nitrotyrosine (Fig-

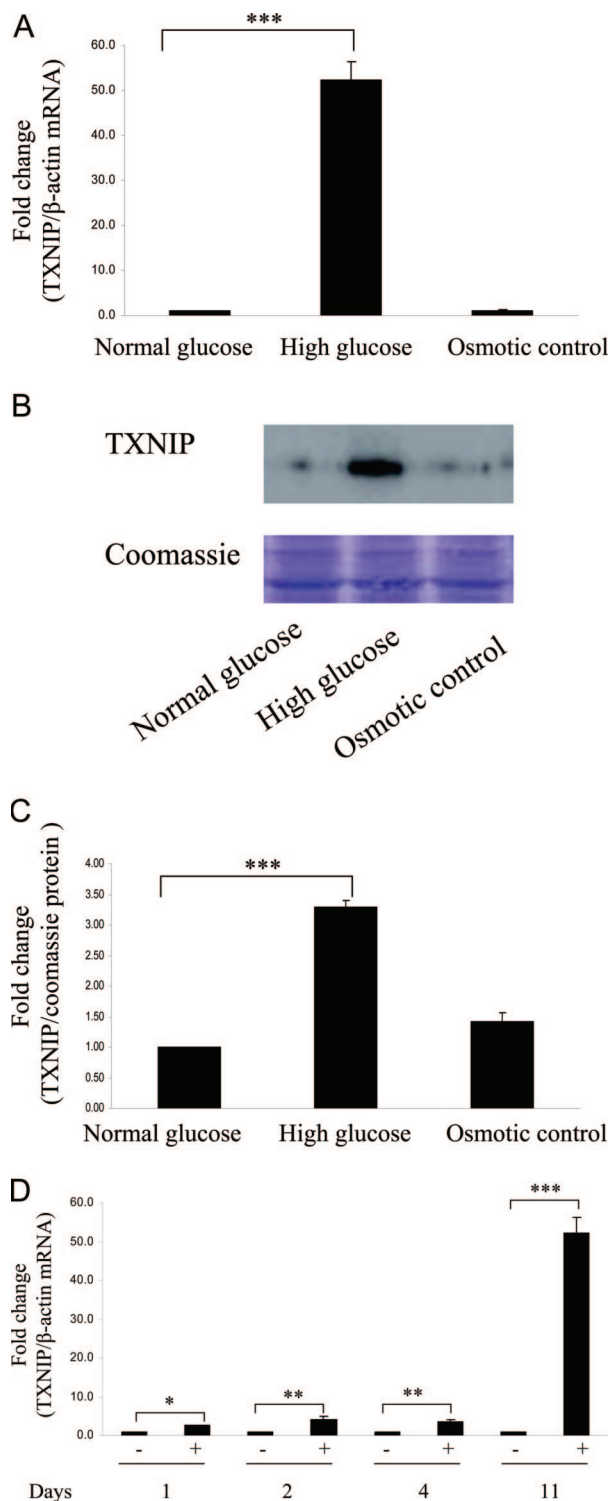


**Figure 1.** High glucose up-regulated Txnip expression in HK-2 cells. HK-2 cells were exposed to 5 mmol/L (normal glucose) and 30 mmol/L (high glucose) D-glucose for 11 days. Thirty mmol/L L-glucose acts as osmotic control. **A:** Real-time RT-PCR was performed, and Txnip mRNA expression was normalized to the housekeeping gene  $\beta$ -actin. Txnip protein expression was measured by Western blotting, and Coomassie Brilliant Blue staining was used as equal loading control. The experiments were repeated three times, with a representative blot shown (**B**), and the densitometry of Western blotting is quantified (**C**). **D:** HK-2 cells were exposed to 5 mmol/L (normal glucose) and 30 mmol/L (high glucose) D-glucose for 1, 2, 4, and 11 days. Txnip and  $\beta$ -actin real-time RT-PCR was performed. Results are mean  $\pm$  SEM and shown as fold change compared with control. \*\*\* $P < 0.0005$ , \*\* $P < 0.005$ , \* $P < 0.05$ ;  $n = 3$ .

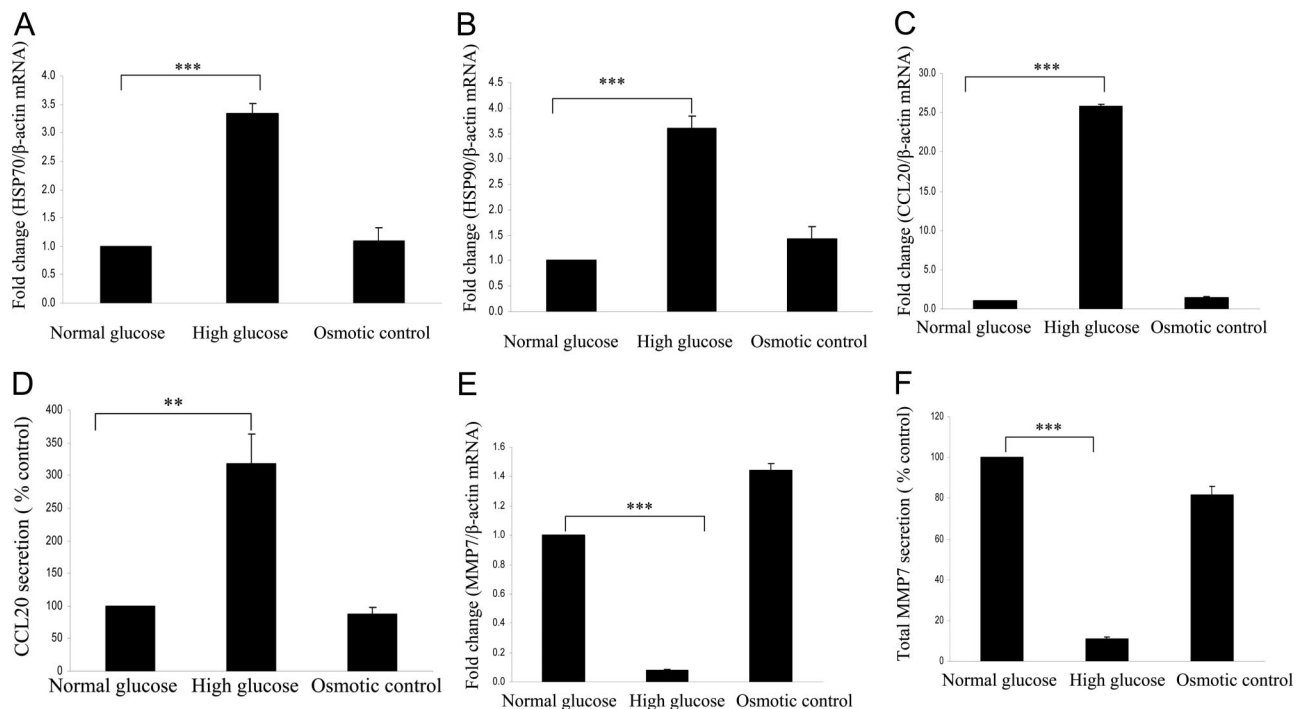


**Figure 2.** High glucose significantly regulated mRNA and protein expression of HSP70, HSP90, CCL20, and MMP7 after HK-2 cells were exposed to high glucose for 11 days. HK-2 cells were exposed to 5 mmol/L (normal glucose) and 30 mmol/L (high glucose) D-glucose for 11 days. Thirty mmol/L L-glucose acts as osmotic control. Real-time RT-PCR was performed, and HSP70 (A), HSP90 (B), CCL20 (C), and MMP7 (E) mRNA expressions were normalized to the housekeeping gene  $\beta$ -actin. Supernatant was collected as described in Materials and Methods, and CCL20 (D) and MMP7 (F) proteins were measured using enzyme-linked immunosorbent assay. Results are mean  $\pm$  SEM and shown as fold change compared with control. \*\*\* $P < 0.0005$ , \*\* $P < 0.005$ ;  $n = 3$ .

ure 3A) and Txnip (Figure 3B) protein were significantly elevated in the diabetic Ren-2 rats (II) compared with nondiabetic control rats (I). Both ROS and Txnip-positive staining increased in dilated tubules in diabetic group compared with nondiabetic groups (Figure 3, C and D). Txnip protein expression in the whole rat kidney tissue measured by Western blotting significantly increased in diabetic rats compared with nondiabetic rats (Figure 3, E and F).

### High Glucose Induced Txnip Expression through a TGF- $\beta$ 1-Independent Pathway

Exposure of HK-2 cells to TGF- $\beta$ 1 significantly decreased Txnip mRNA levels occurring from day 1 and sustaining through day 6 (all  $P < 0.0005$ ) (Figure 4A). In contrast, reduction of Txnip protein expression was not observed until day 2 and sustained at day 6 (Figure 4, B and C). TGF- $\beta$ 1 gene was effectively silenced in HK-2 cells using siRNA technology as previously described.<sup>16</sup> Txnip mRNA

expression significantly increased by 21-fold in TGF- $\beta$ 1-silenced cells ( $P < 0.0005$ ) (Figure 5A). However, the increased level of Txnip returned to control (nonspecific siRNA) level after the addition of pan-specific TGF- $\beta$ -neutralizing antibody in TGF- $\beta$ 1-silenced cells (Figure 5, B and C), suggesting TGF- $\beta$ 2 or -3 might increase in TGF- $\beta$ 1-silenced cells and these two isoforms subsequently increased Txnip expression. We have previously demonstrated the increased levels of TGF- $\beta$ 2 and -3 in TGF- $\beta$ 1-silenced cells result in overexpression of fibronectin.<sup>16</sup> High-glucose exposure for 72 hours further increased Txnip expression by 3.5-fold in TGF- $\beta$ 1-silenced cells compared with wild-type cells ( $P < 0.0005$ ) (Figure 5D), which is consistent with Txnip protein expression by Western blotting (Figure 5, E and F). These data suggest that high glucose induced Txnip expression through a TGF- $\beta$ 1-independent pathway. Moreover, Txnip expression was negatively regulated by TGF- $\beta$ 1 in HK-2 cells.

**Table 3.** Comparison of Gene Expression Levels in Microarray Analysis and Real-Time RT-PCR

Gene name	Fold change in microarray	Fold change in real-time RT-PCR
<i>Txnip</i>	$\uparrow$ 11.5	$\uparrow$ 52.3
<i>HSP70</i>	$\uparrow$ 2.8	$\uparrow$ 3.3
<i>HSP90</i>	$\uparrow$ 2.3	$\uparrow$ 3.6
<i>CCL20</i>	$\uparrow$ 5.2	$\uparrow$ 25.8
<i>MMP-7</i>	$\downarrow$ 4.5	$\downarrow$ 10.0

### Txnip Promoter Activity

Exposure of HK-2 cells to high glucose significantly increased Txnip promoter activity, which peaked at 24 hours ( $P < 0.0005$ ) and sustained at 72 hours ( $P < 0.05$ ) (Figure 6A). In contrast, exposure to the osmotic control (30 mmol/L L-glucose) for 24 hours did not increase Txnip promoter activity ( $1.11 \pm 0.06$ -fold versus normal glucose). Exposure of HK-2 cells to TGF- $\beta$ 1 significantly decreased Txnip promoter activity from 8 hours ( $P < 0.05$ ) to 48 hours (all  $P < 0.0005$ ) (Figure 6B). Txnip promoter activity significantly

**Table 4.** Animal Characteristics

Groups	<i>n</i>	Body weight (g)	Blood glucose (mmol/L)	HbA1c (%)	AER (mg/24 hours)	SBP (mmHg)
Control (Ren-2)	16	289 ± 5.0	6.7 ± 0.15	3.4 ± 0.09	14 ± 1.2	218 ± 7
Diabetic (Ren-2)	14	213 ± 8.0*	31.9 ± 0.59*	11.2 ± 0.25*	81 ± 1.3 <sup>†</sup>	211 ± 8

Values are expressed as means ± SEM.

\**P* < 0.05 versus Ren-2 control.

increased in TGF-β1 silenced cells (*P* < 0.005), and high-glucose exposure for 24 hours further increased promoter activity by 1.43-fold in TGF-β1-silenced cells compared with wild-type cells (*P* < 0.05) (Figure 6C). These data further

demonstrate that high glucose induced Txnip through a TGF-β1-independent pathway and Txnip is negatively regulated by TGF-β1. Promoter assay was used as a means of measuring the promoter response in cells. Its activity does

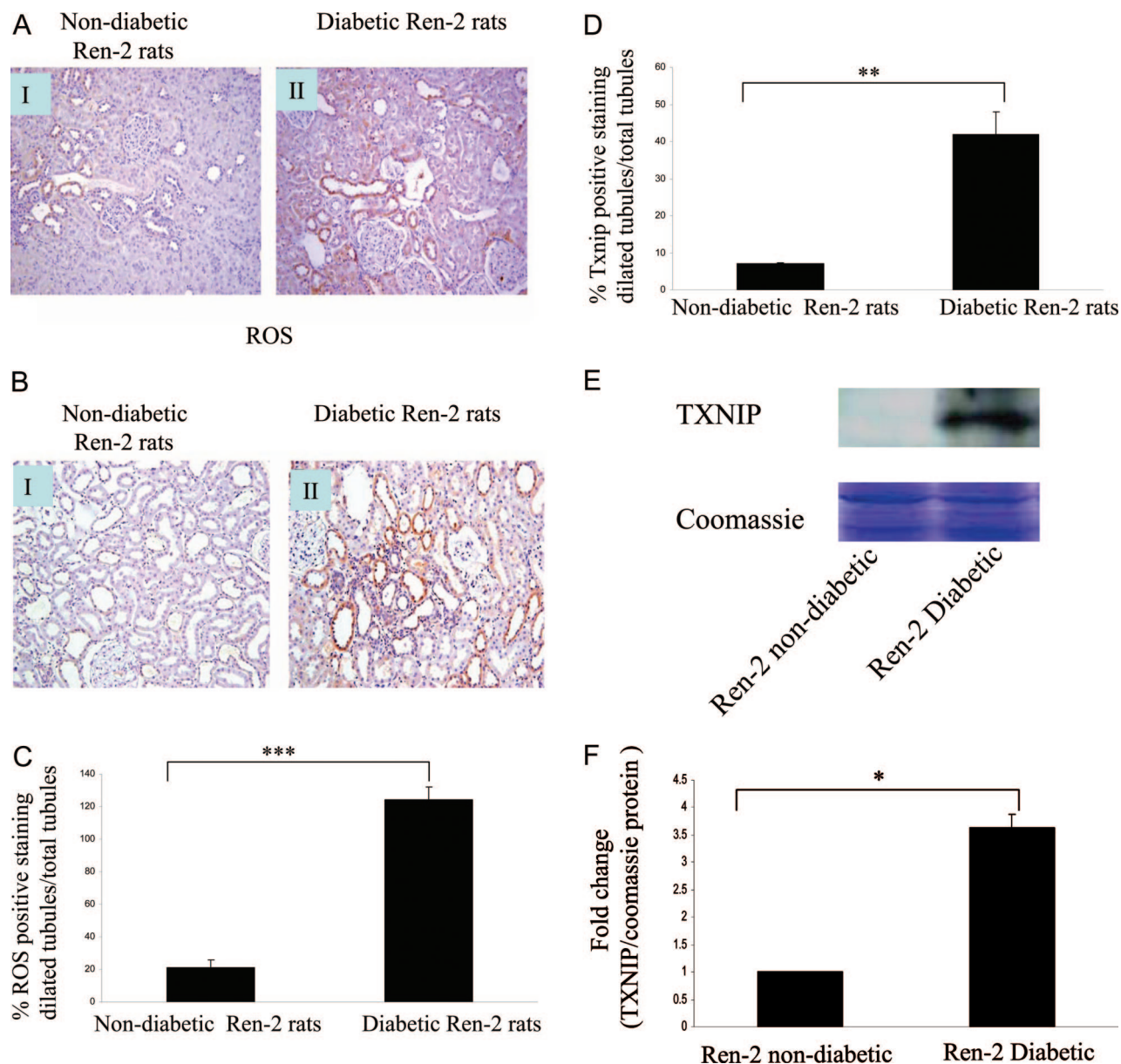


**Figure 3.** Nitrotyrosine and Txnip expression in nondiabetic and diabetic Ren-2 rats. Diabetic Ren-2 rats (II) were associated with an increase in nitrotyrosine (A) and Txnip (B) immunostaining within the tubules when compared with nondiabetic Ren-2 rats (I). Positive staining of nitrotyrosine (ROS) (C) and Txnip (D) in the dilated tubules in nondiabetic and diabetic Ren-2 rats was counted separately and normalized to the number of tubules counted in each chosen field. The data were expressed as percentage of positive staining of ROS or Txnip in dilated tubules per total tubules. Txnip protein in whole rat kidney tissue was measured by Western blotting, and Coomassie Brilliant Blue staining was used as equal loading control (E and F). Results are mean ± SEM and shown as fold change compared with control. \*\*\**P* < 0.0005, \*\**P* < 0.005, \**P* < 0.05; *n* = 3. Original magnifications, ×340 (A and B).

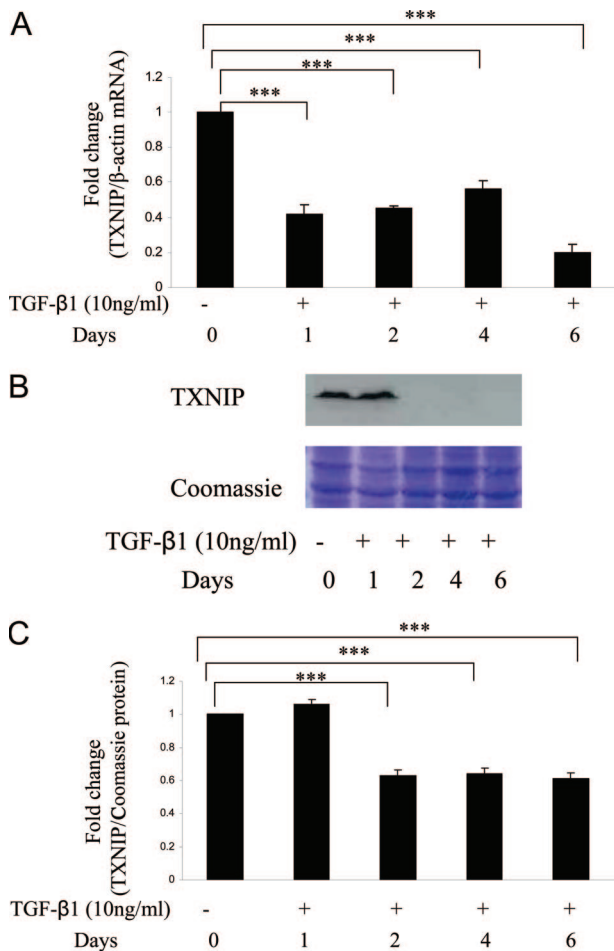


**Figure 4.** The effect of TGF- $\beta$ 1 on Txnip expression in HK-2 cells. HK-2 cells were exposed to 10 ng/ml TGF- $\beta$ 1 for 0, 1, 2, 4, and 6 days. **A:** RNA was collected for measurement of Txnip by real-time RT-PCR and normalized to the housekeeping gene  $\beta$ -actin. **B** and **C:** Txnip protein was measured by Western blotting, and Coomassie Brilliant Blue staining was used as equal loading control. Results are mean  $\pm$  SEM and shown as fold change compared with control. \*\*\* $P$  < 0.0005;  $n$  = 3.

not reflect a consequent linear response for mRNA and protein levels because mRNA production is also affected by many factors such as posttranscription regulation, and multiple factors subsequently regulate protein production and degradation. However, and importantly, the data for Txnip promoter activity are confirmed to be statistically significant and support the Txnip mRNA and protein expression data.

### Discussion

This study has identified by cDNA microarray analysis the specific transcriptional profile of genes directly regulated by high glucose in a model of human proximal tubular cells. In addition to a striking up-regulation of both Txnip and HSP70 and HSP90, we have demonstrated up-regulation of the chemokine CCL20 and down-regulation of the regulator of matrix turnover MMP-7. Importantly, we have demonstrated that the mRNA expression levels of five chosen genes for real-time RT-PCR verification were all consistent with microarray analysis, which confirms the validity of the microarray data.

Txnip, HSP70, and HSP90 are stress-related genes that have previously been reported to be increased in the kidneys of experimental models of diabetic nephropathy.<sup>6,17,18</sup> The present *in vitro* studies confirm that this up-regulation is attributable to high glucose, either directly or via downstream metabolic derangements. Furthermore our studies in an *in vivo* model of diabetic nephropathy localize Txnip up-regulation and associated oxidative stress to the dilated tubules.

The induction of Txnip by high glucose has been reported in primary cultured human mesangial cells and intact human pancreatic islets.<sup>6,19</sup> Minn and colleagues<sup>20</sup> have demonstrated a distinct carbohydrate response element in the human Txnip promoter sufficient to cause glucose responsiveness. Similarly, Txnip has been shown to be increased in streptozotocin-induced diabetic mice, suggesting that diabetes induced alterations in redox imbalance may cause dysregulation of collagen synthesis, contributing to a variety of pathological processes, including the fibrogenic process in diabetic nephropathy.<sup>6</sup> In the diabetic Ren-2 rat, a model of progressive diabetic nephropathy, we detected increased levels of Txnip and oxidative stress in dilated tubules. Much evidence has accumulated to confirm that high glucose induces TGF- $\beta$ 1 in kidney tubule cells.<sup>4,21,22</sup> Although high glucose significantly up-regulates Txnip, unexpectedly, our data demonstrate that TGF- $\beta$ 1 decreases Txnip expression in HK-2 cells. Consistent with this observation, effective silencing of TGF- $\beta$ 1 in proximal tubular cells leads to an enhancement of Txnip expression. We have recently demonstrated that increased TGF- $\beta$ 2 and TGF- $\beta$ 3 expression in TGF- $\beta$ 1-silenced cells results in a paradoxical increase in fibronectin expression.<sup>16</sup> We hypothesize that overexpression of Txnip in TGF- $\beta$ 1-silenced cells is caused by the previously confirmed increase in expression of TGF- $\beta$ 2 and TGF- $\beta$ 3,<sup>16</sup> which in turn increases Txnip expression. Indeed, we have confirmed this hypothesis by the addition of pan-specific TGF- $\beta$ -neutralizing antibody to TGF- $\beta$ 1-silenced cells and increased level of Txnip returned to control level. Hence these data suggest that high glucose induces Txnip through a TGF- $\beta$ 1-independent pathway and that TGF- $\beta$ 1 may act to limit the response to oxidative stress. Kobayashi and colleagues<sup>6</sup> have previously reported in human mesangial cells that high glucose induces Txnip, and overexpression of Txnip increases collagen expression, which was only partially mediated through a TGF- $\beta$ -dependent mechanism. This suggests TGF- $\beta$ 1 might play different roles in the cascade of high glucose-Txnip-collagen type IV induction. In contrast to our data, reports in nonepithelial cells demonstrated that TGF- $\beta$ 1 up-regulated Txnip in murine lung fibroblasts and HL-60 cells, suggesting that the effect of TGF- $\beta$ 1 on Txnip expression is dependent on the cell type studied.<sup>11,22</sup> All TGF- $\beta$  isoforms (TGF- $\beta$ 1, -2, and -3) have been previously reported to have fibrogenic effects on renal cells. TGF- $\beta$ 2 has been reported to induce fibronectin, collagen type I, and collagen type IV in both human retinal pigment epithelial cell line and cultured human optic nerve head astrocytes.<sup>23,24</sup> TGF- $\beta$ 3 has also been reported to decrease matrix metalloproteinase-2 (MMP-2) and increase tissue inhibitor of metalloproteinase-1 (TIMP-1) and collagen type I in primary lung fibroblasts.<sup>25</sup> All three TGF- $\beta$  isoforms have



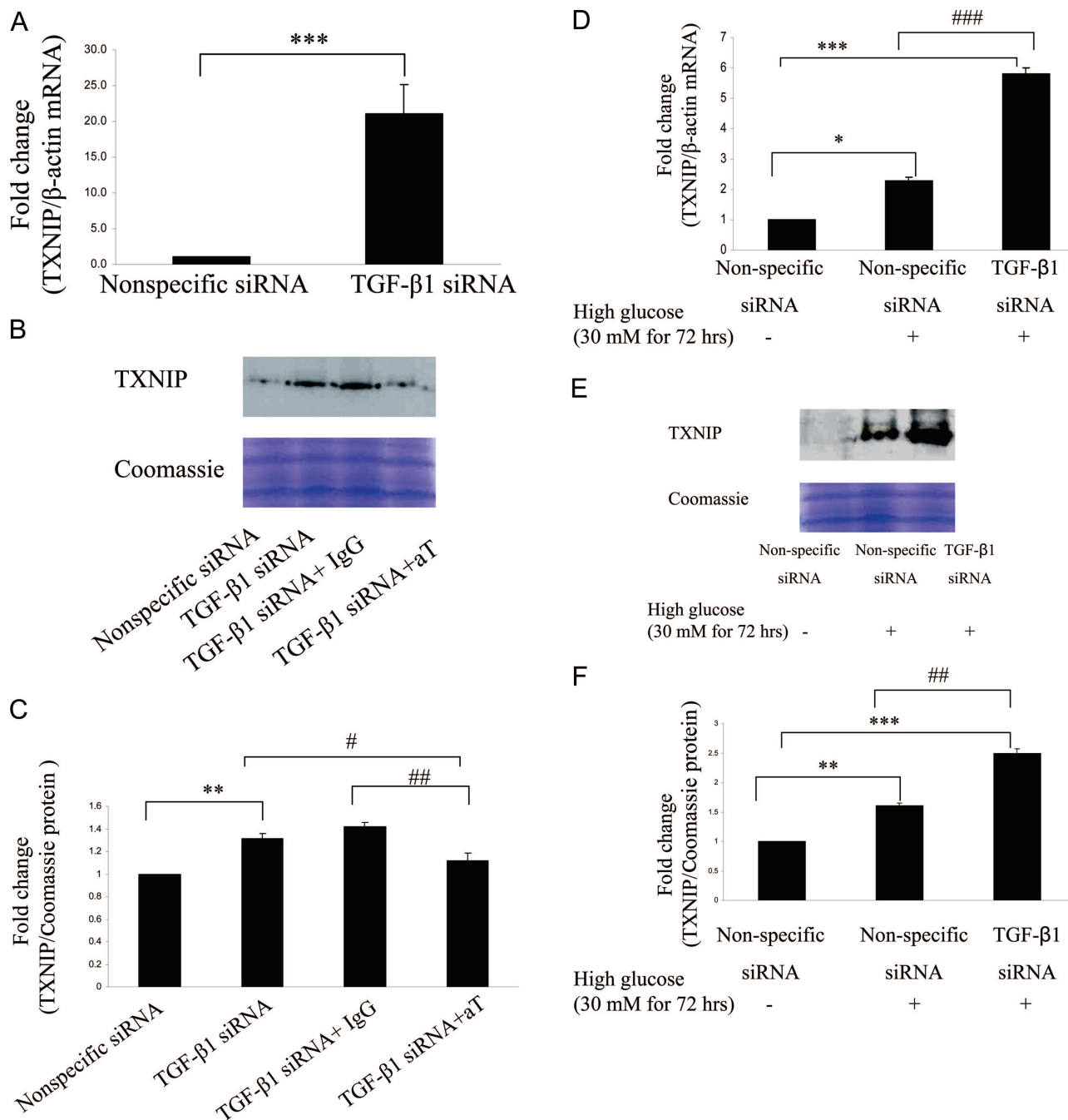


**Figure 5.** The role of TGF-β1 on Txnip expression under high-glucose conditions. Thirty nmol/L of nonspecific or TGF-β1 siRNAs were introduced into HK-2 cells, respectively, at subconfluence using Lipofectamine 2000. Cells were then treated with or without 30 mmol/L D-glucose (HG) for 72 hours. **A** and **D**: RNA was collected for measurement of Txnip mRNA expression. TGF-β1-silenced cells were either exposed to 30 μg/ml of pan-specific TGF-β antibody (aT) or 30 μg/ml rabbit IgG (negative control) or treated with or without HG. **B**, **C**, **E**, and **F**: Txnip protein was measured by Western blotting, and Coomassie Brilliant Blue staining was used as equal loading control. Results are mean ± SEM and are shown as fold change. \*\*\**P* < 0.0005, \*\**P* < 0.005, \**P* < 0.05, ###*P* < 0.0005, ##*P* < 0.005, #*P* < 0.05; *n* = 3.

been reported to activate the TGF-β signaling pathway via Smad2 activation.<sup>26–29</sup> However, the differential effects of these three TGF-β isoforms on Txnip expression are still unknown.

We and others have previously demonstrated that high glucose is an inducer of many chemokines such as interleukin-8, MCP-1, and transcription factors such as nuclear factor-κB and AP-1.<sup>4,30,31</sup> This is the first report, to our knowledge, suggesting that CCL20 is up-regulated

by high glucose. CCL20 is an important chemokine that plays a key role in the regulation of dendritic cell trafficking, and recruitment and activation of T cells.<sup>32</sup> It is produced by activated cells, including monocytes, T cells, endothelial cells, and fibroblasts. Although previously demonstrated to be up-regulated in response to inflammatory stimuli in epithelial cells, the present study demonstrates it to be up-regulated in response to high glucose.

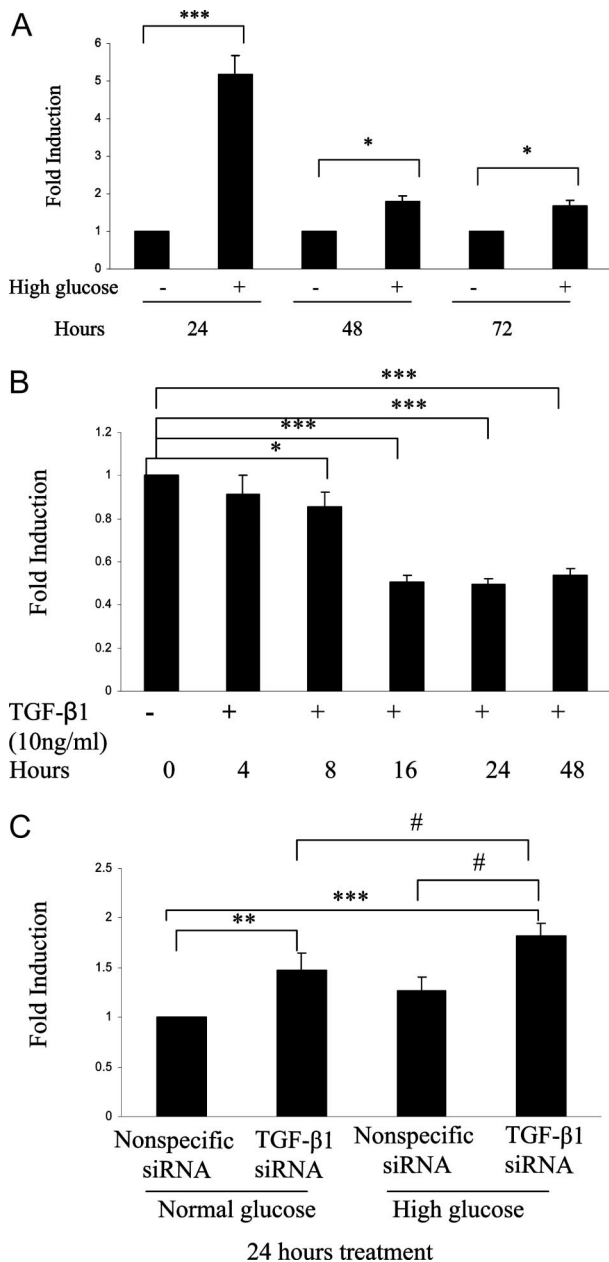


**Figure 6.** The role of TGF-β1 on Txnip promoter activity under high-glucose conditions. HK-2 cells were 85% subconfluent when seeded on a 24-well plate and transfected with 2 μg of Txnip promoter pGL3 (Firefly) and 1 ng of pRL-SV40 (Renilla) using Lipofectamine 2000. **A:** Cells were maintained in medium containing 5 and 30 mmol/L D-glucose for 24, 48, and 72 hours after 6 hours of transfection. Cell lysate was then collected for Txnip promoter assay. **B:** HK-2 cells were exposed to 10 ng/ml TGF-β1 for 0, 4, 8, 16, 24, and 48 hours, and cell lysate was then collected for Txnip promoter assay. Thirty nmol/L of nonspecific or TGF-β1 siRNAs were introduced into HK-2 cells at subconfluence using Lipofectamine 2000. **C:** Cells were then treated with or without 30 mmol/L D-glucose (HG) for 24 hours, and cell lysate was then collected for Txnip promoter assay. Firefly luciferase activity was normalized to Renilla, which serves as internal control. All results are mean ± SEM and are shown as fold change. \*\*\**P* < 0.0005, \*\**P* < 0.005, \**P* < 0.05, #*P* < 0.05; *n* = 3.

HSP70 and HSP90 are molecular chaperones expressed constitutively under normal conditions to maintain protein homeostasis and are induced when subjected to environmental stress.<sup>33</sup> The biological functions of HSP70/HSP90 go beyond their chaperone activity. They are essential for the maturation and inactivation of nuclear hormones and

other signaling molecules<sup>33,34</sup> and play a role in vesicle formation and protein trafficking.<sup>35</sup> HSP90 is one of the most abundant proteins of eukaryotic cells, and it comprises 1 to 2% of total proteins under nonstress conditions. It is essential for cell survival. Some reports suggest that induction of HSP70 protects against the deleterious consequences of chronic diseases such as diabetic kidney diseases.<sup>36</sup> Previous reports have suggested that high glucose increased HSP90-α in cultured cells, and diabetes increased the amount of HSP90-α on the luminal surface of the aorta.<sup>17</sup> Hence, the observed up-regulation of HSP70 and HSP90 in response to high-glucose conditions was not unexpected in our tubular cell model.

PAI-1 was also significantly up-regulated by high glucose in the microarray analysis, which we have previously confirmed in human proximal tubular cells.<sup>37</sup> PAI-1 has been shown to increase in kidneys of humans and animals with diabetes mellitus and contribute to diabetic nephropathy by regulating TGF-β and renal extracellular matrix production.<sup>38</sup>

The microarray analysis and subsequent real-time RT-PCR confirmed that MMP-7 (also known as PUMP-1 or matrilysin) was down-regulated under high-glucose conditions. It is well known that MMP-2 and MMP-9 are involved in matrix regulation in kidney diseases.<sup>39,40</sup> However, the role of MMP-7 has not been previously been studied in diabetic nephropathy. MMP-7 is expressed in epithelial cells of normal and diseased tissues and is implicated in normal and pathological tissue remodeling processes.<sup>41</sup> MMP-7 is capable of digesting a large series of proteins of the extracellular matrix such as collagen IV, gelatins, laminin, aggrecan, entactin, elastin, and versican. It activates other proteinases such as urokinase plasminogen activator and pro-MMP-1, -2, -9, and cleaves additional substrates such as osteopontin.<sup>41,42</sup> Down-regulation under hyperglycemic conditions suggests that MMP-7 plays an important, but to date unidentified, role in diabetic nephropathy.

In summary, these studies have importantly demonstrated the transcriptional profile of genes up-regulated in the kidney proximal tubule by high glucose. The up-regulation of Txnip protein and concomitant oxidative stress was confirmed in an *in vivo* model of diabetes mellitus. The up-regulation of Txnip has been shown to be clearly independent of TGF-β1 in high-glucose conditions. Furthermore, TGF-β1 is demonstrated to regulate negatively Txnip expression. The studies have demonstrated the up-regulation of the chemokine CCL20 and the down-regulation of MMP-7, together potentially promote the inflammatory and profibrotic components of diabetic nephropathy.

## References

- Gilbert RE, Cooper ME: The tubulointerstitium in progressive diabetic kidney disease: more than an aftermath of glomerular injury? *Kidney Int* 1999, 56:1627–1637
- Phillips AO, Steadman R: Diabetic nephropathy: the central role of renal proximal tubular cells in tubulointerstitial injury. *Histol Histopathol* 2002, 17:247–252
- Kobayashi T, Inoue T, Okada H, Kikuta T, Kanno Y, Nishida T, Takigawa M, Sugaya T, Suzuki H: Connective tissue growth factor medi-

- ates the profibrotic effects of transforming growth factor- $\beta$  produced by tubular epithelial cells in response to high glucose. *Clin Exp Nephrol* 2005, 9:114–121
4. Panchapakesan U, Pollock CA, Chen XM: The effect of high glucose and PPAR-gamma agonists on PPAR- $\gamma$  expression and function in HK-2 cells. *Am J Physiol* 2004, 287:F528–F534
  5. Schulze PC, Yoshioka J, Takahashi T, He Z, King GL, Lee RT: Hyperglycemia promotes oxidative stress through inhibition of thioredoxin function by thioredoxin-interacting protein. *J Biol Chem* 2004, 279:30369–30374
  6. Kobayashi T, Uehara S, Ikeda T, Itadani H, Kotani H: Vitamin D3 up-regulated protein-1 regulates collagen expression in mesangial cells. *Kidney Int* 2003, 64:1632–1642
  7. Nishiyama A, Matsui M, Iwata S, Hirota K, Masutani H, Nakamura H, Takagi Y, Sono H, Gon Y, Yodoi J: Identification of thioredoxin-binding protein-2/vitamin D(3) up-regulated protein 1 as a negative regulator of thioredoxin function and expression. *J Biol Chem* 1999, 274:21645–21650
  8. Kelly DJ, Skinner SL, Gilbert RE, Cox AJ, Cooper ME, Wilkinson-Berka JL: Effects of endothelin or angiotensin II receptor blockade on diabetes in the transgenic (mRen-2)27 rat. *Kidney Int* 2000, 57:1882–1894
  9. Qi W, Chen X, Polhill TS, Sumual S, Twigg S, Gilbert RE, Pollock CA: Transforming growth factor- $\beta$ 1 induces interleukin-8 and macrophage chemoattractant protein-1 through a connective tissue growth factor independent pathway. *Am J Physiol* 2006, 290:F703–F709
  10. Chen S, Hoffman BB, Lee JS, Kasama Y, Jim B, Kopp JB, Ziyadeh FN: Cultured tubule cells from TGF- $\beta$ 1 null mice exhibit impaired hypertrophy and fibronectin expression in high glucose. *Kidney Int* 2004, 65:1191–1204
  11. Han SH, Jeon JH, Ju HR, Jung U, Kim KY, Yoo HS, Lee YH, Song KS, Hwang HM, Na YS, Yang Y, Lee KN, Choi I: VDUP1 upregulated by TGF- $\beta$ 1 and 1,25-dihydroxyvitamin D3 inhibits tumor cell growth by blocking cell-cycle progression. *Oncogene* 2003, 22:4035–4046
  12. Rhyu DY, Yang Y, Ha H, Lee GT, Song JS, Uh ST, Lee HB: Role of reactive oxygen species in TGF- $\beta$ 1-induced mitogen-activated protein kinase activation and epithelial-mesenchymal transition in renal tubular epithelial cells. *J Am Soc Nephrol* 2005, 16:667–675
  13. Yoon YS, Lee JH, Hwang SC, Choi KS, Yoon G: TGF $\beta$ 1 induces prolonged mitochondrial ROS generation through decreased complex IV activity with senescent arrest in Mv1Lu cells. *Oncogene* 2005, 24:1895–1903
  14. Pfaffl MW: A new mathematical model for relative quantification in real-time RT-PCR. *Nucleic Acids Res* 2001, 29:e45
  15. Gilbert RE, Wilkinson-Berka JL, Johnson DW, Cox A, Soulis T, Wu LL, Kelly DJ, Jerums G, Pollock CA, Cooper ME: Renal expression of transforming growth factor- $\beta$  inducible gene-h3 ( $\beta$ ig-h3) in normal and diabetic rats. *Kidney Int* 1998, 54:1052–1062
  16. Qi W, Chen X, Holian J, Mreich E, Twigg S, Gilbert RE, Pollock CA: Transforming growth factor-beta1 differentially mediates fibronectin and inflammatory cytokine expression in kidney tubular cells. *Am J Physiol* 2006, 291:F1070–F1077
  17. Lei H, Romeo G, Kazlauskas A: Heat shock protein 90 $\alpha$ -dependent translocation of annexin II to the surface of endothelial cells modulates plasmin activity in the diabetic rat aorta. *Circ Res* 2004, 94:902–909
  18. Zhang Y, Wada J, Hashimoto I, Eguchi J, Yasuhara A, Kanwar YS, Shikata K, Makino H: Therapeutic approach for diabetic nephropathy using gene delivery of translocase of inner mitochondrial membrane 44 by reducing mitochondrial superoxide production. *J Am Soc Nephrol* 2006, 17:1090–1101
  19. Shalev A, Pise-Masison CA, Radonovich M, Hoffmann SC, Hirshberg B, Brady JN, Harlan DM: Oligonucleotide microarray analysis of intact human pancreatic islets: identification of glucose-responsive genes and a highly regulated TGF $\beta$  signaling pathway. *Endocrinology* 2002, 143:3695–3698
  20. Minn AH, Hafele C, Shalev A: Thioredoxin-interacting protein is stimulated by glucose through a carbohydrate response element and induces  $\beta$ -cell apoptosis. *Endocrinology* 2005, 146:2397–2405
  21. Danda RS, Habiba NM, Rincon-Choles H, Bhandari BK, Barnes JL, Abboud HE, Pergola PE: Kidney involvement in a nongenetic rat model of type 2 diabetes. *Kidney Int* 2005, 68:2562–2571
  22. Zhu Y, Casado M, Vaulont S, Sharma K: Role of upstream stimulatory factors in regulation of renal transforming growth factor- $\beta$ 1. *Diabetes* 2005, 54:1976–1984
  23. Fuchshofer R, Birke M, Welge-Lüssen U, Kook D, Lutjen-Drecoll E: Transforming growth factor- $\beta$ 2 modulated extracellular matrix component expression in cultured human optic nerve head astrocytes. *Invest Ophthalmol Vis Sci* 2005, 46:568–578
  24. Saika S, Yamanaka O, Ikeda K, Kim-Mitsuyama S, Flanders KC, Yoo J, Roberts AB, Nishikawa-Ishida I, Ohnishi Y, Muragaki Y, Ooshima A: Inhibition of p38MAP kinase suppresses fibrotic reaction of retinal pigment epithelial cells. *Lab Invest* 2005, 85:838–850
  25. Papakonstantinou E, Aletas AJ, Roth M, Tamm M, Karakiulakis G: Hypoxia modulates the effects of transforming growth factor-beta isoforms on matrix-formation by primary human lung fibroblasts. *Cytokine* 2003, 24:25–35
  26. Molin DG, Poelmann RE, DeRuiter MC, Azhar M, Doetschman T, Gittenberger-de Groot AC: Transforming growth factor  $\beta$ -SMAD2 signaling regulates aortic arch innervation and development. *Circ Res* 2004, 95:1109–1117
  27. Hartner A, Hilgers KF, Bitzer M, Veelken R, Schocklmann HO: Dynamic expression patterns of transforming growth factor- $\beta$ (2) and transforming growth factor- $\beta$  receptors in experimental glomerulonephritis. *J Mol Med* 2003, 81:32–42
  28. Cui XM, Chai Y, Chen J, Yamamoto T, Ito Y, Bringas P, Shuler CF: TGF- $\beta$ 3-dependent SMAD2 phosphorylation and inhibition of MEE proliferation during palatal fusion. *Dev Dyn* 2003, 227:387–394
  29. Chaturvedi K, Sarkar DK: Role of protein kinase C-Ras-MAPK p44/42 in ethanol and transforming growth factor- $\beta$ 3-induced basic fibroblast growth factor release from folliculostellate cells. *J Pharmacol Exp Ther* 2005, 314:1346–1352
  30. Chow FY, Nikolic-Paterson DJ, Ozols E, Atkins RC, Rollin BJ, Tesch GH: Monocyte chemoattractant protein-1 promotes the development of diabetic renal injury in streptozotocin-treated mice. *Kidney Int* 2006, 69:73–80
  31. Srinivasan S, Bolick DT, Hatley ME, Natarajan R, Reilly KB, Yeh M, Chrestensen C, Sturgill TW, Hedrick CC: Glucose regulates interleukin-8 production in aortic endothelial cells through activation of the p38 mitogen-activated protein kinase pathway in diabetes. *J Biol Chem* 2004, 279:31930–31936
  32. Dieu MC, Vanbervliet B, Vicari A, Bridon JM, Oldham E, Ait-Yahia S, Briere F, Zlotnik A, Lebecque S, Caux C: Selective recruitment of immature and mature dendritic cells by distinct chemokines expressed in different anatomic sites. *J Exp Med* 1998, 188:373–386
  33. Nollen EA, Morimoto RI: Chaperoning signaling pathways: molecular chaperones as stress-sensing 'heat shock' proteins. *J Cell Sci* 2002, 115:2809–2816
  34. Pratt WB, Toft DO: Regulation of signaling protein function and trafficking by the hsp90/hsp70-based chaperone machinery. *Exp Biol Med* (Maywood) 2003, 228:111–133
  35. Young JC, Barral JM, Ulrich Hartl F: More than folding: localized functions of cytosolic chaperones. *Trends Biochem Sci* 2003, 28:541–547
  36. Söti C, Nagy E, Giricz Z, Vigh L, Csermely P, Ferdinandy P: Heat shock proteins as emerging therapeutic targets. *Br J Pharmacol* 2005, 146:769–780
  37. Qi W, Poronnik P, Young B, Jackson CJ, Field MJ, Pollock CA: Human cortical fibroblast responses to high glucose and hypoxia. *Nephron Physiol* 2004, 96:p121–p129
  38. Nicholas SB, Aguiniga E, Ren Y, Kim J, Wong J, Govindarajan N, Noda M, Wang W, Kawano Y, Collins A, Hsueh WA: Plasminogen activator inhibitor-1 deficiency retards diabetic nephropathy. *Kidney Int* 2005, 67:1297–1307
  39. McLennan SV, Death AK, Fisher EJ, Williams PF, Yue DK, Turtle JR: The role of the mesangial cell and its matrix in the pathogenesis of diabetic nephropathy. *Cell Mol Biol (Noisy-le-grand)* 1999, 45:123–135
  40. McLennan SV, Fisher E, Martell SY, Death AK, Williams PF, Lyons JG, Yue DK: Effects of glucose on matrix metalloproteinase and plasmin activities in mesangial cells: possible role in diabetic nephropathy. *Kidney Int Suppl* 2000, 77:S81–S87
  41. Wilson CL, Matrisian LM: Matrilysin: an epithelial matrix metalloproteinase with potentially novel functions. *Int J Biochem Cell Biol* 1996, 28:123–136
  42. Agnihotri R, Crawford HC, Haro H, Matrisian LM, Havrda MC, Liaw L: Osteopontin, a novel substrate for matrix metalloproteinase-3 (stromelysin-1) and matrix metalloproteinase-7 (matrilysin). *J Biol Chem* 2001, 276:28261–28267